Mass uncertainties of $f_0(600)$ and $f_0(1370)$ and their effects on determination of the quark and glueball admixtures of the $I = 0$ scalar mesons

Amir H. Fariborz*

Department of Mathematics/Science, State University of New York Institute of Technology, Utica, New York 13504-3050, USA

(Received 7 July 2006; published 21 September 2006)

Within a nonlinear chiral Lagrangian framework, the correlations between the quark and glueball admixtures of the isosinglet scalar mesons below 2 GeV and the current large uncertainties on the masses of $f_0(600)$ and $f_0(1370)$ are studied. The framework is formulated in terms of two scalar meson nonets (a two-quark nonet and a four-quark nonet) together with a scalar glueball. It is shown that, while some properties of these states are sensitive to the masses of $f_0(600)$ and $f_0(1370)$, several relatively robust conclusions can be made: $f_0(600)$, $f_0(980)$, and $f_0(1370)$ are admixtures of two- and four-quark components, with $f_0(600)$ being dominantly a nonstrange four-quark state, and $f_0(980)$ and $f_0(1370)$ having a dominant two-quark component. Similarly, $f_0(1500)$ and $f_0(1710)$ have considerable two- and four-quark admixtures, but in addition they have a large glueball component. For each state, a detailed analysis providing the numerical estimates of all components is given. It is also shown that this framework clearly favors the experimental values: $m^{\text{expt}}[f_0(600)] < 700$ MeV and $m^{\text{expt}}[f_0(1370)] =$ 1300–1450 MeV. Moreover, an overall fit to the available data shows a reciprocal substructure for $f_0(600)$ and $f_0(1370)$, and a linear correlation between their masses of the form $m[f_0(1370)] = 0.29m[f_0(600)] + 1.22$ GeV. The scalar glueball mass of 1.5–1.7 GeV is found in this analysis.

DOI: 10.1103/PhysRevD.74.054030 PACS numbers: 13.75.Lb, 11.15.Pg, 11.80.Et, 12.39.Fe

I. INTRODUCTION

Exploring the properties of the scalar mesons is known to be a nontrivial task in low-energy QCD. This is due to issues such as their large decay widths and overlap with the background, as well as having several decay channels over a tight energy range [1]. Particularly, the case of $I = 0$ states is even more complex due to their various mixings, for example, among two- and four-quark states and scalar glueballs. Below 1 GeV, the well-established experimental states are as follows[1]: $f_0(980)$ [$I = 0$] and $a_0(980)$ [$I = 1$], together with states that have uncertain properties; $f_0(600)$ or σ [$I = 0$] with a mass of 400–1200 MeV, and a decay width of 600–1000 MeV; and $K_0^*(800)$ or κ [$I = 1/2$] which is not yet listed but cautiously discussed by PDG. The existence of the $K_0^*(800)$ has been confirmed in some investigations [2–6], while it has been disputed in some other approaches [7,8]. In the range of 1–2 GeV, the listed scalar states are as follows [1]: $K_0^*(1430)$ [$I = 1/2$]; $a_0(1450)$ [$I = 1$]; and $f_0(1370)$, $f_0(1500)$, $f_0(1710)$ [$I = 0$]. The isodoublet and isotriplet states are generally believed to be closer to $q\bar{q}$ objects, even though some of their properties significantly deviate from such a description. Among the heavier isosinglet states, $f_0(1370)$ has the largest experimental uncertainty [1] on its mass (1200–1500 MeV) and decay width (200–500 MeV), and other states in the energy range of around 1.5 GeV (or above) seem to contain a large glue component and may be good candidates for the lowest scalar glueball state.

A simple quark-antiquark description is known to fail for the lowest-lying scalar states, and that has made them the focus of intense investigation for a long time. Several foundational scenarios for their substructures have been considered, including the MIT bag model [9], the $K\bar{K}$ molecule [10], and the unitarized quark model [11], and many theoretical frameworks for the properties of the scalars have been developed, including, among others, the chiral Lagrangian of Refs. [12–24], upon which the present investigation is based. Many recent works [25–49] have investigated different aspects of the scalar mesons, particularly, their family connections and possible description in terms of meson nonet(s), which provide a comparison with this work.

Various ways of grouping the scalars together have been considered in the literature [37–49]. For example, in some approaches, the properties of the scalars above 1 GeV (independent of the states below 1 GeV) are investigated, whereas other works have only focused on the states below 1 GeV. There are also works that have investigated several possibilities for grouping together some of the states above 1 GeV with those below 1 GeV.

In addition to various ways that the physical states may be grouped together, different bases out of quark-antiquark, four-quark, and glueball states have been considered for their internal structure. For example, in a number of investigations the $I = 0$ states above 1 GeV are studied within a framework which incorporates quark-antiquark and glueball components. However, with the lack of a complete framework for understanding the properties of the scalar mesons, it seems more objective to develop general frameworks in which, *a priori*, no specific substructure for the scalars is assumed, and, instead, all possible components (quark-antiquark, four-quark, and glueball) are considered. The framework of the

*Email address: fariboa@sunyit.edu

present work considers all such components for the $I = 0$ states, and studies the five listed $I = 0$ states below 2 GeV [1].

Besides the generality of the framework, there are supportive indications that the lowest-lying and the next-to-lowest-lying scalar states have admixtures of quark-antiquark and four-quark components. For example, it is shown in [17] that $a_0(1450)$ and $K_0^*(1430)$ have considerable two- and four-quark admixtures, which provides a basis for explaining the mass spectrum and the partial decay widths of the $I = 1/2$ and $I = 1$ scalars [$K_0^*(800)$, $a_0(980)$, $K_0^*(1430)$, and $a_0(1450)$]. It then raises the question that, if the $I = 1/2$ and $I = 1$ scalars below 2 GeV are admixtures of two- and four-quark components, why should the $I = 0$ states not be blurred with such a mixing complexity? Answering this question is the main motivation of this paper, and we will see that this framework shows that there is a substantial admixture of the two-quark and the four-quark components for the $I = 0$ scalars below 2 GeV.

Motivated by the importance of the mixing for the $I = 1/2$ and $I = 1$ in this framework, the case of the $I = 0$ states was initially studied in [22,23] in which mixing with a scalar glueball is also included. In [22] the parameter space of the $I = 0$ Lagrangian, which is already constrained by the properties of the $I = 1/2$ and $I = 1$ states in Ref. [17], is studied using the mass spectrum and several two-pseudoscalar decay widths and decay ratios of the $I = 0$ states. The present work extends the work of [22] by investigating in detail the effect of the mass uncertainties of $f_0(600)$ and $f_0(1370)$ on the components of the $I = 0$ states below 2 GeV. It also provides an insight into the likelihood of the masses of $f_0(600)$ and $f_0(1370)$ within their experimental values [1] in the ranges 400–1200 MeV and 1200–1500 MeV, respectively. In addition, a linear correlation between these two masses is predicted by the model.

Specifically, we will numerically analyze the mass spectrum and perform an inverse problem: knowing the mass of the physical states [or in the case of $f_0(600)$ and $f_0(1370)$ a wide experimental range for their masses), we search for the parameter space of the Lagrangian (which is formulated in terms of a two-quark nonet and a four-quark nonet) and find solutions that can reproduce these masses. Once the parameter space is determined, it provides information about the properties of the two nonets. The results are summarized in Fig. 1. We will show how the present model describes the $I = 0$ scalar states in terms of a four-quark nonet N which lies in the range of 0.83–1.24 GeV, together with a two-quark nonet N' in the 1.24–1.38 GeV range, and a scalar glueball that this model predicts in the range of 1.5–1.7 GeV (Fig. 1). The mass range of the two-quark scalar nonet N' is qualitatively consistent with the expected range of 1.2 GeV from spectroscopy of p-wave mesons. We will see that this analysis shows that, similar to the case

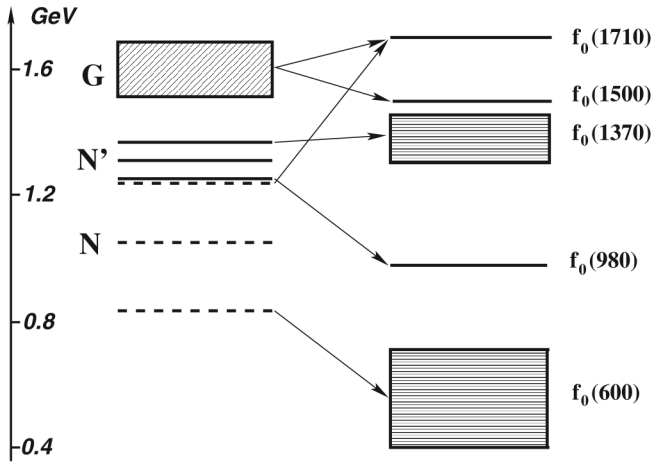

FIG. 1. Prediction of the present model for the formation of the $I = 0$ scalar states below 2 GeV. On the right, the physical states are shown, with the solid lines representing the experimentally well-established masses, and the height of the two boxes representing the prediction of the present model for the uncertainties of the masses of $f_0(600)$ and $f_0(1370)$, which are approximately in the ranges 0.4–0.7 GeV and 1.3–1.45 GeV, respectively. On the left, the bare states are shown, with the dashed lines representing the four-quark nonet N, the solid lines representing the two-quark nonet N', and the box representing the scalar glueball. The masses of the bare states in the two nonets (from bottom to top) are $m(\bar{u}\,\bar{d}\,ud) = 0.83$ GeV, $m(\bar{d}\,\bar{s}\,ud) = 1.06$ GeV, $m((\bar{s}\,\bar{d}\,ds + \bar{s}\,\bar{u}\,us)/\sqrt{2}) = m((\bar{u}u + \bar{d}d)/\sqrt{2}) = 1.24$ GeV, $m(\bar{u}s) = 1.31$ GeV, and $m(\bar{s}s) = 1.38$ GeV. The uncertainty of the glueball mass (shown by the height of the box, approximately between 1.5 GeV and 1.7 GeV) is due to the uncertainty of the masses of $f_0(600)$ and $f_0(1370)$. The arrows show the dominant component(s) of each physical state. More details are given in Figs. 7 and 8.

of $I = 1/2$ and $I = 1$ scalar mesons, the $I = 0$ scalars have significant admixtures of two- and four-quark components, and in addition $f_0(1500)$ and $f_0(1710)$ have a dominant glueball content. The dominant component(s) of each state is summarized in Fig. 1.

The underlying framework of the present work has previously been applied in analyzing numerous low-energy processes that involve scalar mesons, and consistent pictures have emerged. The existence of $f_0(600)$ (or σ) and $K_0^*(800)$ (or κ) and their properties have been investigated in Refs. [12,13]. The lowest-lying nonet of scalars and a four-quark interpretation of these states are studied in [14] and applied to $\pi\eta$ scattering in [16] and to several decays such as $\eta' \to \eta\pi\pi$ [15] and $\eta \to 3\pi$ [21], and radiative ϕ decays [19]. In addition to Ref. [17], the mixing between a two-quark nonet and a four-quark nonet is also investigated in [18,24].

We describe the theoretical framework in Sec. II, followed by the numerical results in Sec. III, and a short summary in Sec. IV.

II. THEORETICAL FRAMEWORK

A. Mixing mechanism for $I = 1/2$ and $I = 1$ scalar states

In Ref. [17] the properties of the $I = 1/2$ and $I = 1$ scalar mesons, $K_0^*(800)$, $K_0^*(1430)$, $a_0(980)$, and $a_0(1450)$, in a nonlinear chiral Lagrangian framework are studied in detail. In this approach, a $\bar{q}\,\bar{q}\,qq$ nonet N mixes with a $\bar{q}q$ nonet N' and provides a description of the mass spectrum and decay widths of these scalars. $K_0^*(1430)$ and $a_0(1450)$ are generally believed to be good candidates for a $\bar{q}q$ nonet [1], but some of their properties do not quite follow this scenario. For example, in a $\bar{q}q$ nonet, the isotriplet is expected to be lighter than the isodoublet, but for these two states [1],

$$m[a_0(1450)] = 1474 \pm 19 \text{ MeV} > m[K_0^*(1430)] = 1412 \pm 6 \text{ MeV}. \tag{1}$$

Also, their decay ratios given by PDG [1] do not follow a pattern expected from an SU(3) symmetry (given in parentheses):

$$\begin{aligned} \frac{\Gamma[a_0^{\text{total}}]}{\Gamma[K_0^* \to \pi K]} &= 0.92 \pm 0.12 \ (1.51), \\ \frac{\Gamma[a_0 \to K\bar{K}]}{\Gamma[a_0 \to \pi\eta]} &= 0.88 \pm 0.23 \ (0.55), \\ \frac{\Gamma[a_0 \to \pi\eta']}{\Gamma[a_0 \to \pi\eta]} &= 0.35 \pm 0.16 \ (0.16). \end{aligned} \tag{2}$$

These properties of $K_0^*(1430)$ and $a_0(1450)$ are naturally explained by the mixing mechanism of Ref. [17]. The general mass terms for the $I = 1/2$ and the $I = 1$ states can be written as

$$\begin{aligned} \mathcal{L}_{\text{mass}}^{I=1/2,1} = &-a\,\text{Tr}(NN) - b\,\text{Tr}(NN\mathcal{M}) - a'\,\text{Tr}(N'N') \\ &- b'\,\text{Tr}(N'N'\mathcal{M}) \end{aligned} \tag{3}$$

where $\mathcal{M} = \text{diag}(1, 1, x)$ with x being the ratio of the strange to nonstrange quark masses; a, b, a', and b' are unknown parameters fixed by the unmixed or "bare" masses (denoted below by the subscript "0"):

$$\begin{aligned} m^2[a_0] &= 2(a+b), \quad m^2[a_0'] = 2(a'+b'), \\ m^2[K_0] &= 2a + (1+x)b, \quad m^2[K_0'] = 2a' + (1+x)b'. \end{aligned} \tag{4}$$

As N is a four-quark nonet and N' a two-quark nonet, we expect

$$m^2[K_0] < m^2[a_0] \leq m^2[a_0'] < m^2[K_0']. \tag{5}$$

In fact, this is how we tag N and N' to a four-quark nonet and a two-quark nonet, respectively. Introducing a general mixing

$$\mathcal{L}_{\text{mix}}^{I=1/2,1} = -\gamma\,\text{Tr}(NN'), \tag{6}$$

it is shown in [17] that, for $0.51 < \gamma < 0.62$ GeV^2, it is possible to recover the physical masses such that the bare masses have the expected ordering of (5). In this mechanism, the bare isotriplet states split more than the isodoublets, and, consequently, the physical isovector state $a_0(1450)$ becomes heavier than the isodoublet state $K_0^*(1430)$, in agreement with the observed experimental values in (1). The light isovector and isodoublet states are $a_0(980)$ and $K_0^*(800)$. With the physical masses $m[a_0(980)] = 0.9835$ GeV, $m[K_0^*(800)] = 0.875$ GeV, $m[a_0(1450)] = 1.455$ GeV, and $m[K_0(1430)] = 1.435$ GeV, the best values of the mixing parameter γ and the bare masses are found in [17]

$$\begin{aligned} m_{a_0} = m_{a_0'} &= 1.24 \text{ GeV}, \quad m_{K_0} = 1.06 \text{ GeV}, \\ m_{K_0'} &= 1.31 \text{ GeV}, \quad \gamma = 0.58 \text{ GeV}^2. \end{aligned} \tag{7}$$

These parameters are then used to study the decay widths of the $I = 1/2$ and $I = 1$ states [17]. A general Lagrangian describing the coupling of the two nonets N and N' to two-pseudoscalar particles is introduced and the unknown Lagrangian parameters are found by fits to various decay widths.

In summary, the work of Ref. [17] clearly shows that properties of the lowest and the next-to-lowest $I = 1/2$ and $I = 1$ scalar states can be described by a mixing between a quark-antiquark nonet and a four-quark nonet. It is concluded that the $I = 1$ states are close to maximal mixing [i.e. $a_0(980)$ and $a_0(1450)$ are approximately made of 50% quark-antiquark and 50% four-quark components], and the $I = 1/2$ states have a similar structure with $K_0^*(800)$ made of approximately 74% four-quark and 26% quark-antiquark components, with the reverse structure for $K_0^*(1430)$. Now, if the lowest and the next-to-lowest $I = 1/2$ and $I = 1$ states have a substantial mixing of quark-antiquark and four-quark components, then it seems necessary to investigate a similar scenario for the $I = 0$ scalars, which, in addition, can have a glueball component as well. In other words, if the lowest and the next-to-lowest scalars are going to be grouped together, then all of the quark-antiquark, four-quark, and glueball components for the $I = 0$ states should be taken into account. The case of $I = 0$ states will be discussed in the next section.

B. Isosinglet states

The $I = 0$ scalars have been investigated in many recent works (see, for example, Refs. [40,41,43–45,47,49]) including the general approach with two- and four-quark components as well as a glueball component of Refs. [22,23]. Within the framework of Ref. [17], an initial analysis is given in [22] in which the mass and the decay Lagrangian for the $I = 0$ scalar mesons are studied in some detail. The general mass terms for nonets N and N', and a scalar glueball G can be written as

$$\mathcal{L}^{I=0}_{\text{mass}} = \mathcal{L}^{I=1/2,1}_{\text{mass}} - c\,\text{Tr}(N)\,\text{Tr}(N) - d\,\text{Tr}(N)\,\text{Tr}(N\mathcal{M}) - c'\,\text{Tr}(N')\,\text{Tr}(N') - d'\,\text{Tr}(N')\,\text{Tr}(N'\mathcal{M}) - gG^2. \tag{8}$$

The unknown parameters c and d induce "internal" mixing between the two $I = 0$ flavor combinations [$(N^1_1 + N^2_2)/\sqrt{2}$ and N^3_3] of nonet N. Similarly, c' and d' play the same role in nonet N'. Parameters c, d, c', and d' do not contribute to the mass spectrum of the $I = 1/2$ and $I = 1$ states. The last term represents the glueball mass term. The term $\mathcal{L}^{I=1/2,1}_{\text{mass}}$ is imported from Eq. (3) together with its parameters from Eq. (7).

The mixing between N and N', and the mixing of these two nonets with the scalar glueball G can be written as

$$\mathcal{L}^{I=0}_{\text{mix}} = \mathcal{L}^{I=1/2,1}_{\text{mix}} - \rho\,\text{Tr}(N)\,\text{Tr}(N') - eG\,\text{Tr}(N) - fG\,\text{Tr}(N') \tag{9}$$

where the first term is given in (6) with γ from (7). The second term does not contribute to the $I = 1/2$, 1 mixing, and in the special limit of $\rho \to -\gamma$,

$$-\gamma\,\text{Tr}(NN') - \rho\,\text{Tr}(N)\,\text{Tr}(N') = \gamma\epsilon^{abc}\epsilon_{ade}N^d_b N'^e{}_c \tag{10}$$

which is more consistent with the Okubo-Zweig-Iizuka rule than the individual γ and ρ terms and is studied in [40]. Here we do not restrict the mixing to this particular combination and, instead, take ρ as an *a priori* unknown free parameter. Terms with unknown couplings e and f describe mixing with the scalar glueball G. As a result, the five isosinglets below 2 GeV become a mixture of five

$$\mathbf{M}^2 = \begin{bmatrix} 2m^2_{K_0} - m^2_{a_0} + 2(c + dx) & \sqrt{2}[2c + (1 + x)d] \\ \sqrt{2}[2c + (1 + x)d] & m^2_{a_0} + 4(c + d) \\ \gamma + \rho & \sqrt{2}\rho \\ \sqrt{2}\rho & \gamma + 2\rho \\ e & \sqrt{2}e \end{bmatrix}$$

$$\begin{bmatrix} \gamma + \rho & \sqrt{2}\rho & e \\ \sqrt{2}\rho & \gamma + 2\rho & \sqrt{2}e \\ 2m^2_{K'_0} - m^2_{a'_0} + 2(c' + d'x) & \sqrt{2}[2c' + (1 + x)d'] & f \\ \sqrt{2}[2c' + (1 + x)d'] & m^2_{a'_0} + 4(c' + d') & \sqrt{2}f \\ f & \sqrt{2}f & 2g \end{bmatrix} \tag{14}$$

in which the value of the unmixed $I = 1/2$, 1 masses, and the mixing parameter γ are substituted in from (7). We see that there are eight unknown parameters in (14) which are c, d, c', d', g, ρ, e, and f. We will use a numerical analysis to search this eight dimensional parameter space for the best values that give the closest agreement with experimentally known masses. Particularly, we will study in detail the effect of the large uncertainties on the masses of $f_0(600)$ and $f_0(1370)$ on the resulting parameters.

III. MATCHING THE THEORETICAL PREDICTION TO EXPERIMENTAL DATA

To determine the eight unknown Lagrangian parameters (c, c', d, d', e, f, g, and ρ), we input the experimental masses of the scalar states. Out of the five isosinglet states, three have a well-established experimental mass [1]:

$$\begin{aligned} m^{\text{expt}}[f_0(980)] &= 980 \pm 10\ \text{MeV}, \\ m^{\text{expt}}[f_0(1500)] &= 1507 \pm 5\ \text{MeV}, \\ m^{\text{expt}}[f_0(1710)] &= 1713 \pm 6\ \text{MeV}. \end{aligned} \tag{15}$$

However, the experimental masses of $f_0(600)$ and $f_0(1370)$ have very large uncertainties [1]:

$$\begin{aligned} m^{\text{expt}}[f_0(600)] &= 400 \to 1200\ \text{MeV}, \\ m^{\text{expt}}[f_0(1370)] &= 1200 \to 1500\ \text{MeV}. \end{aligned} \tag{16}$$

We search for the eight Lagrangian parameters [which, in

different flavor combinations, and their masses can be organized as

$$\mathcal{L}^{I=0}_{\text{mass}} + \mathcal{L}^{I=0}_{\text{mix}} = -\tfrac{1}{2}\tilde{\mathbf{F}}_0\mathbf{M}^2\mathbf{F}_0 = -\tfrac{1}{2}\tilde{\mathbf{F}}\mathbf{M}^2_{\text{diag}}\mathbf{F} \tag{11}$$

with

$$\mathbf{F}_0 = \begin{pmatrix} N^3_3 \\ (N^1_1 + N^2_2)/\sqrt{2} \\ N'^3_3 \\ (N'^1_1 + N'^2_2)/\sqrt{2} \\ G \end{pmatrix} = \begin{pmatrix} \bar{u}\,\bar{d}\,ud \\ (\bar{s}\,\bar{d}\,ds + \bar{s}\,\bar{u}\,us)/\sqrt{2} \\ \bar{s}s \\ (\bar{u}u + \bar{d}d)/\sqrt{2} \\ G \end{pmatrix} = \begin{pmatrix} f^{NS}_0 \\ f^{S}_0 \\ f'^{S}_0 \\ f'^{NS}_0 \\ G \end{pmatrix} \tag{12}$$

where the superscripts NS and S respectively represent the nonstrange and strange combinations. $\mathbf{F}$ contains the physical fields,

$$\mathbf{F} = \begin{pmatrix} \sigma(550) \\ f_0(980) \\ f_0(1370) \\ f_0(1500) \\ f_0(1710) \end{pmatrix} = K^{-1}\mathbf{F}_0 \tag{13}$$

where K^{-1} is the transformation matrix. The mass squared matrix is

turn, determine the mass matrix (14)] such that three of the resulting eigenvalues match their central experimental values in (15), and the other two masses fall somewhere in the experimental ranges in (16). This means that, out of the five eigenvalues of (14), three (eigenvalues 2, 4, and 5) should match the fixed target values in (15), but two (eigenvalues 1 and 3) have no fixed target values and instead can be matched to any values in (16). Therefore, to include all possibilities for the experimental ranges in (16), we numerically scan the $m^{\text{expt}}[f_0(600)]$–$m^{\text{expt}}[f_0(1370)]$ plane over the allowed ranges, and at each point we fit for the eight Lagrangian parameters such that the three theoretically calculated eigenvalues (2, 4, and 5) match the fixed target masses in (15), and the other two eigenvalues (1 and 3) match the variable target masses at the chosen point in this plane. At a given point in the $m^{\text{expt}}[f_0(600)]$–$m^{\text{expt}}[f_0(1370)]$ plane, we measure the goodness of the fit by the smallness of the quantity

$$\chi(m^{\text{expt}}[f_0(600)], m^{\text{expt}}[f_0(1370)]) = \sum_i \frac{|m_i^{\text{theo}} - m_i^{\text{expt}}|}{m_i^{\text{expt}}} \tag{17}$$

where $i = 1, \ldots, 5$ correspond to the five $I = 0$ states in ascending order (for example, $m_1^{\text{expt}} = m^{\text{expt}}[f_0(600)], \ldots$). The value of $\chi \times 100$ gives the overall percent difference between theory and experiment. A total of 14 641 eight-parameter fits were performed over the target points in the $m^{\text{expt}}[f_0(600)]$–$m^{\text{expt}}[f_0(1370)]$ plane [50]. This procedure creates a three dimensional graph of χ as a function of $m^{\text{expt}}[f_0(600)]$ and $m^{\text{expt}}[f_0(1370)]$. The overall results of the fits for the experimentally allowed range of masses are given in Fig. 2, in which the projections of χ onto the χ–$m^{\text{expt}}[f_0(600)]$ plane and onto the χ–$m^{\text{expt}}[f_0(1370)]$ plane are shown. We can easily see that the experimental mass of $f_0(600)$ above 700 MeV, and the experimental mass of $f_0(1370)$ outside the range of 1300 to 1450 MeV are not favored by this model.

A more refined numerical analysis narrows down the favored regions to the ranges shown in Fig. 3. We see that the lowest value of χ occurs within the ranges

$$\begin{aligned} m^{\text{expt}}[f_0(600)] &= 500 \rightarrow 600 \text{ MeV}, \\ m^{\text{expt}}[f_0(1370)] &= 1350 \rightarrow 1400 \text{ MeV}. \end{aligned} \tag{18}$$

In this region, χ exhibits a series of local minima, also shown in a more refined numerical work in Fig. 4. Although χ has its lowest values in the regions given in (18), we see that it only increases by approximately 0.01 outside of this region and can be comparable to the theoretical uncertainties of this framework. Therefore, for a more conservative estimate, we take into account all local minima with $\chi < 0.02$. This confines the experimental masses to the ranges

$$\begin{aligned} m^{\text{expt}}[f_0(600)] &= 400 \rightarrow 700 \text{ MeV}, \\ m^{\text{expt}}[f_0(1370)] &= 1300 \rightarrow 1450 \text{ MeV}. \end{aligned} \tag{19}$$

The local minima of χ in this range are shown in Fig. 5 in which the projection of χ onto the $m^{\text{expt}}[f_0(600)]$–$m^{\text{expt}}[f_0(1370)]$ plane is given. In the gray region, there is an overall disagreement of less than 5% between theory and experiment. The local minima (with $\chi < 0.02$) are shown with dots, together with a linear fit that shows the correlation between the masses of $f_0(600)$ and $f_0(1370)$:

$$m[f_0(1370)] = 0.29m[f_0(600)] + 1.22 \text{ GeV}. \tag{20}$$

At all local minima (with $\chi < 0.02$), a detailed numerical analysis is performed and the eight Lagrangian parame-

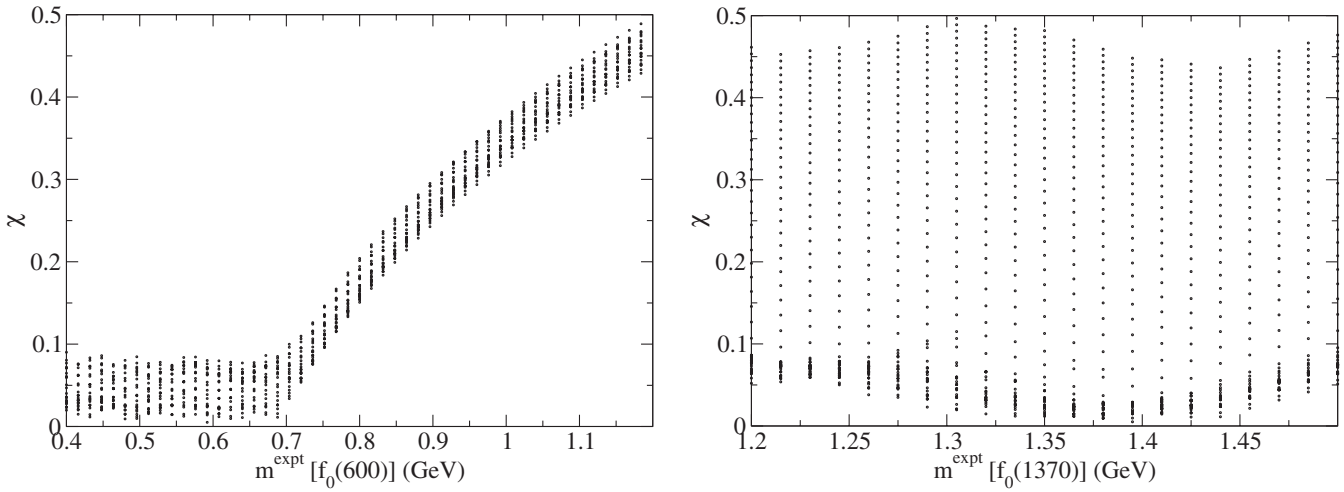

FIG. 2. Projection of χ onto the χ–$m^{\text{expt}}[f_0(600)]$ plane and onto the χ–$m^{\text{expt}}[f_0(1370)]$ plane. The left figure shows that values of $m^{\text{expt}}[f_0(600)] > 700$ MeV result in a significant disagreement between theory and experiment. The right figure shows that $m^{\text{expt}}[f_0(1370)]$ outside of the range 1300–1450 MeV is not favored by the model.

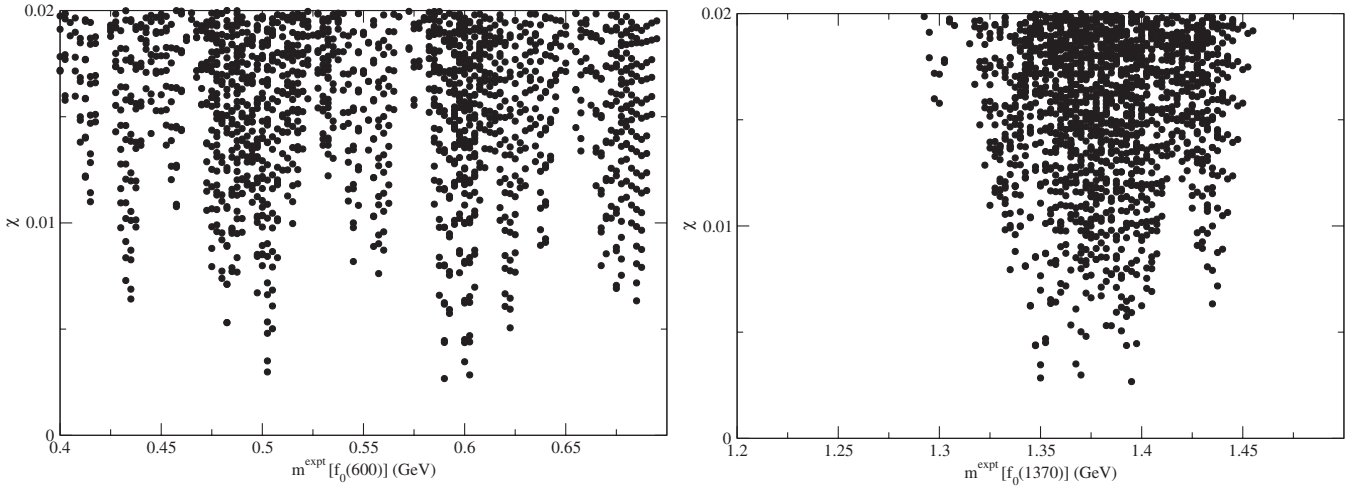

FIG. 3. Projection of χ onto the χ–$m^{\text{expt}}[f_0(600)]$ plane and onto the χ–$m^{\text{expt}}[f_0(1370)]$ plane. The left figure shows a series of local minima in χ with the lowest values in the range 500 MeV $\leq m^{\text{expt}}[f_0(600)] \leq$ 600 MeV. The right figure shows that the present model predicts that $m^{\text{expt}}[f_0(1370)]$ is confined within a smaller range of 1350 MeV to 1400 MeV.

ters are determined. The large uncertainties on $m^{\text{expt}}[f_0(600)]$ and $m^{\text{expt}}[f_0(1370)]$ do not allow an accurate determination of these parameters. In this work we study the correlation between these uncertainties and the determination of the Lagrangian parameters. For orientation, let us first begin by investigating the central values of

$$m^{\text{expt}}[f_0(600)] = 558 \text{ MeV}, \qquad m^{\text{expt}}[f_0(1370)] = 1373 \text{ MeV}. \tag{21}$$

It is important to also notice that the central value of $m[f_0(600)] = 558$ MeV is exactly what was first found in [12] in applying the nonlinear chiral Lagrangian of this work to $\pi\pi$ scattering. At the particular point of (21), the result of the fit is given in Table I, and is consistent with the initial investigation of this model in Ref. [22] in which the effect of the mixing parameter ρ is only studied at several discrete points. The result given in Table I supplements the work of [22] by treating ρ as a general, free parameter. The rotation matrix is

$$K^{-1} = \begin{bmatrix} 0.812 & -0.065 & -0.542 & -0.183 & 0.101 \\ 0.346 & -0.447 & 0.294 & 0.764 & -0.106 \\ 0.418 & 0.198 & 0.768 & -0.328 & 0.299 \\ -0.106 & 0.292 & -0.174 & 0.403 & 0.844 \\ 0.190 & 0.820 & -0.006 & 0.338 & -0.422 \end{bmatrix} \tag{22}$$

which, in turn, determines the quark and glueball components of each physical state as presented in Fig. 6. Several general observations can be made in Fig. 6. Clearly, $f_0(600)$ is dominantly a nonstrange four-quark state with a substantial $\bar{s}s$ component. On the other hand, the dominant structure of $f_0(1370)$ seems to be the reverse of

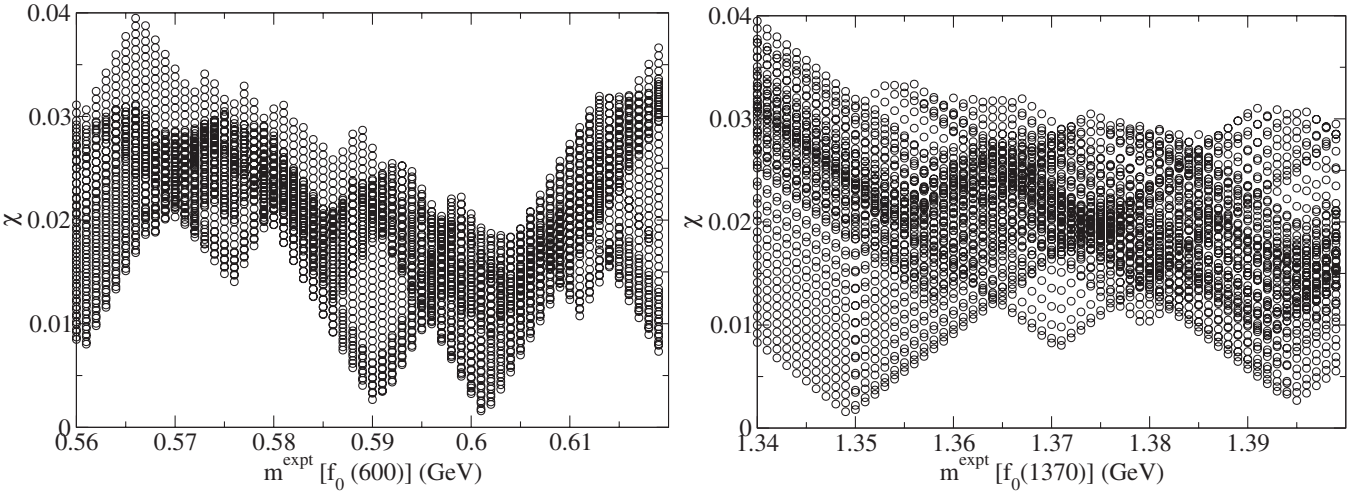

FIG. 4. Projection of χ onto the χ–$m^{\text{expt}}[f_0(600)]$ plane and onto the χ–$m^{\text{expt}}[f_0(1370)]$ plane. χ exhibits a series of local minima.

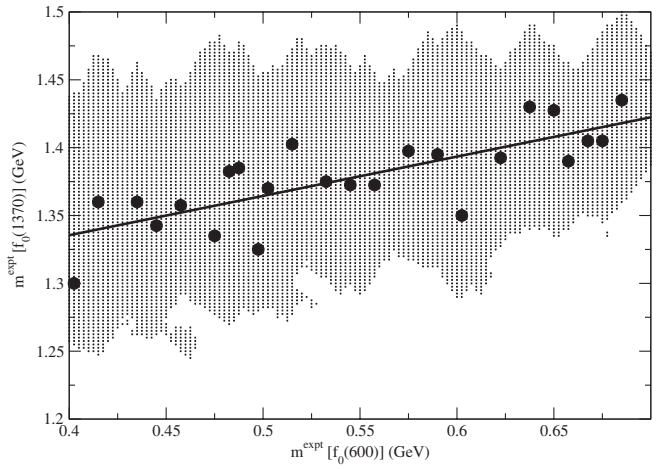

FIG. 5. Projection of χ onto the $m^{\text{expt}}[f_0(600)]$–$m^{\text{expt}}[f_0(1370)]$ plane. In the gray region there is an overall disagreement of less than 5% between theory and experiment. The circles represent points on this plane at which χ has a local minimum and $\chi < 0.02$. The solid line captures the trend of these local minima with the equation $m[f_0(1370)] = 0.29m[f_0(600)] + 1.22$ GeV.

$f_0(600)$. $f_0(980)$ seems to have a dominant nonstrange two-quark component with a significant strange four-quark component. $f_0(1500)$ appears to have a dominant glueball component with some minor two- and four-quark admixtures. The dominant component of $f_0(1710)$ seems to be a strange four-quark state followed by a glueball component.

The scalar glueball mass can be calculated from the fit in Table I:

$$m_G = \sqrt{2g} = 1.52 \text{ GeV} \tag{23}$$

which is in a range expected from lattice QCD [51].

Next we will examine the effect of deviation from the central values of $m^{\text{expt}}[f_0(600)]$ and $m^{\text{expt}}[f_0(1370)]$ on the predictions given in Fig. 6. We will find that the average properties of $f_0(600)$, $f_0(980)$, and $f_0(1370)$ remain close to those given in Fig. 6, but some of the properties of $f_0(1500)$ and $f_0(1710)$ are sensitive to such deviations.

To investigate the effect of the mass uncertainties of $f_0(600)$ and $f_0(1370)$, we perform eight-parameter fits at each of the local minima of Fig. 5, and determine the

TABLE I. Fitted values of the Lagrangian parameters for $m^{\text{expt}}[f_0(600)] = 558$ MeV and $m^{\text{expt}}[f_0(1370)] = 1373$ MeV.

Lagrangian parameters	Fitted values (GeV^2)
c	2.32×10^{-1}
d	-9.11×10^{-3}
c'	-4.29×10^{-3}
d'	-1.25×10^{-2}
g	1.16
ρ	2.87×10^{-2}
e	-2.13×10^{-1}
f	6.10×10^{-2}

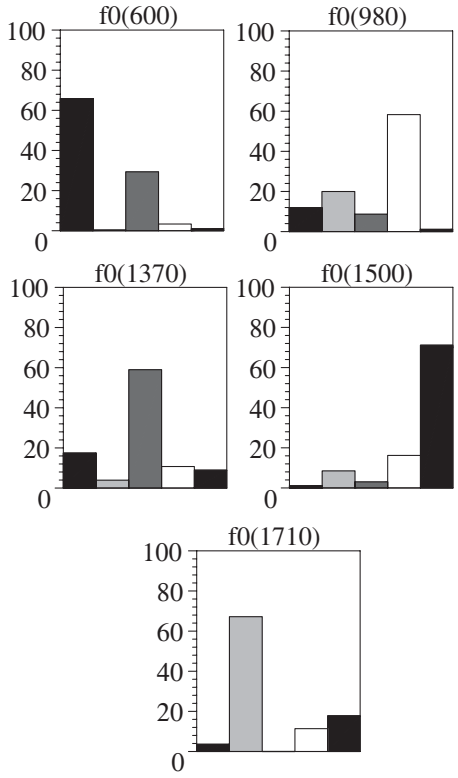

FIG. 6. Percentage of the quark and glueball components of the scalar states for values of $m^{\text{expt}}[f_0(600)] = 558$ MeV and $m^{\text{expt}}[f_0(1370)] = 1373$ MeV. In each figure, the columns from left to right, respectively, represent the percentage of $\bar{u}\,\bar{d}\,ud$ (black), $(\bar{s}\,\bar{d}\,ds + \bar{s}\,\bar{u}\,us)/\sqrt{2}$ (light gray), $\bar{s}s$ (dark gray), $(\bar{u}u + \bar{d}d)/\sqrt{2}$ (white), and glueball (black).

variation of the Lagrangian parameters around the values in Table I. The results are summarized in Table II. We see that, practically, the Lagrangian parameters are quite sensitive to the mass of $f_0(600)$ and $f_0(1370)$. The only exception is the parameter g which determines the glueball mass:

TABLE II. The effect of the uncertainties of $m^{\text{expt}}[f_0(600)]$ and $m^{\text{expt}}[f_0(1370)]$ on the Lagrangian parameters. The averaged value of the parameters (second column) is compared with their (asymmetric) range of variation (third column). Only parameter g (which determines the glueball mass) is relatively insensitive to $m^{\text{expt}}[f_0(600)]$ and $m^{\text{expt}}[f_0(1370)]$.

Lagrangian parameters	Average (GeV^2)	Variation (GeV^2)
c	1.71×10^{-1}	$(0.37 \rightarrow 2.60) \times 10^{-1}$
d	-7.32×10^{-3}	$(-14.44 \rightarrow -2.63) \times 10^{-3}$
c'	-2.87×10^{-3}	$(-5.32 \rightarrow -0.64) \times 10^{-3}$
d'	-0.97×10^{-2}	$(-1.41 \rightarrow -0.27) \times 10^{-2}$
g	1.24	$1.15 \rightarrow 1.44$
ρ	4.7×10^{-2}	$(1.31 \rightarrow 9.14) \times 10^{-2}$
e	-2.10×10^{-1}	$(-3.02 \rightarrow -1.76) \times 10^{-1}$
f	3.74×10^{-2}	$(1.15 \rightarrow 11.40) \times 10^{-2}$

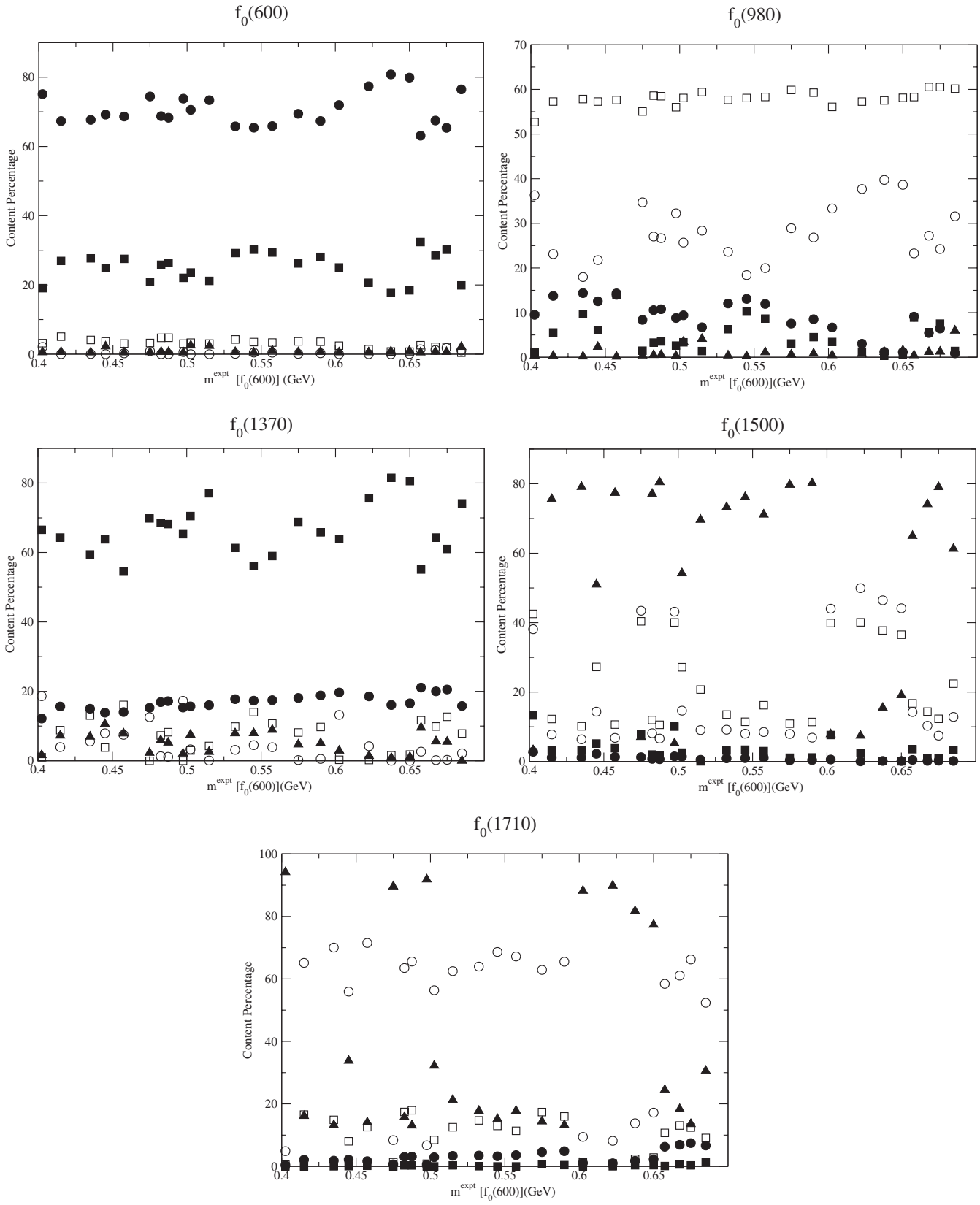

FIG. 7. Percentage of quark and glueball components of the scalar states vs $m^{\text{expt}}[f_0(600)]$: $\bar{u}\,\bar{d}\,ud$ (filled circles), $(\bar{s}\,\bar{d}\,ds + \bar{s}\,\bar{u}\,us)/\sqrt{2}$ (empty circles), $\bar{s}s$ (filled squares), $(\bar{u}u + \bar{d}d)/\sqrt{2}$ (empty squares), and glueball (filled triangles).

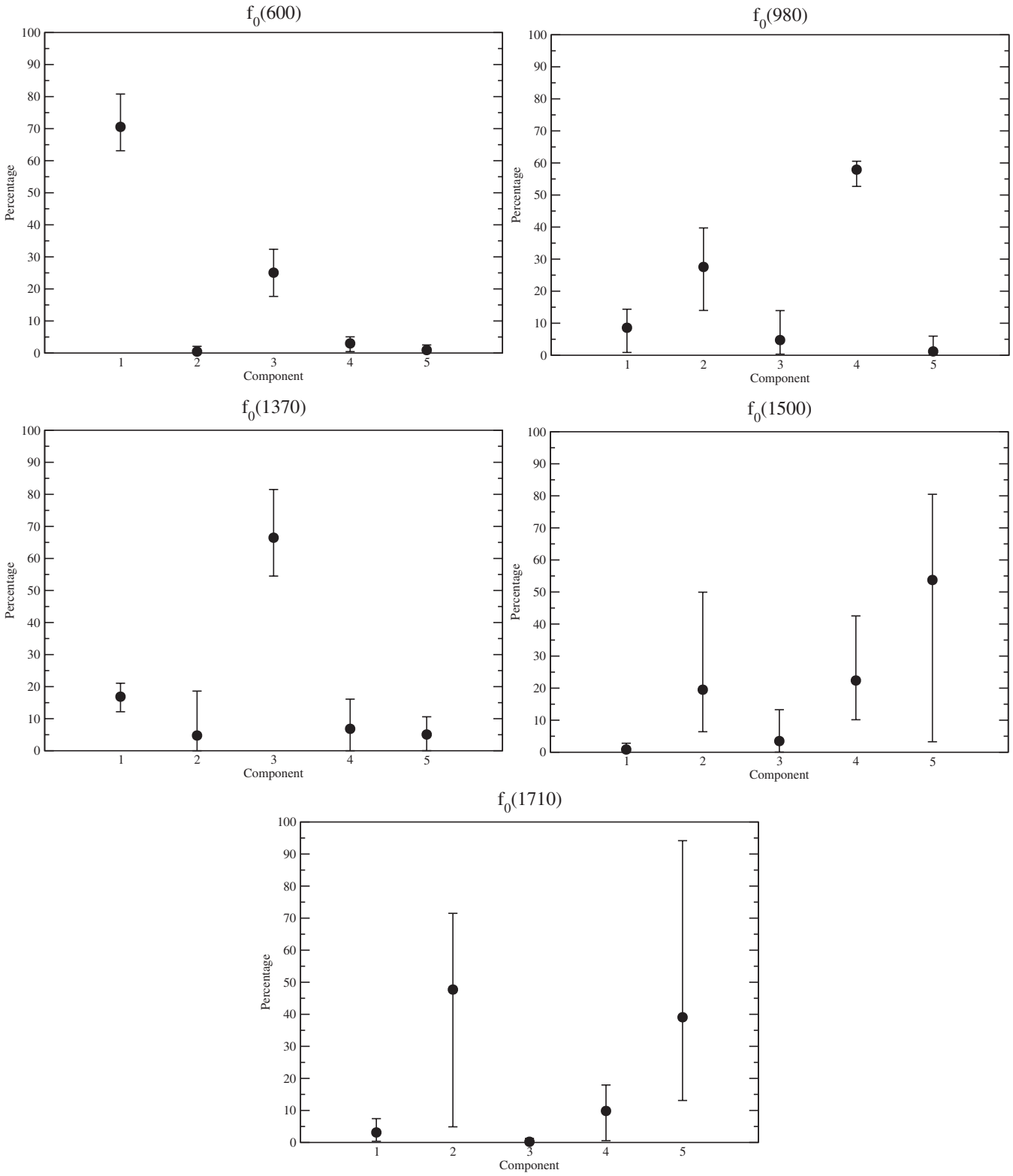

FIG. 8. The effects of the mass uncertainties of $f_0(600)$ and $f_0(1370)$ on the percentage of the quark and glueball components of the scalar states. Components 1 to 5, respectively, represent $\bar{u}\,\bar{d}\,ud$, $(\bar{s}\,\bar{d}\,ds + \bar{s}\,\bar{u}\,us)/\sqrt{2}$, $\bar{s}s$, $(\bar{u}u + \bar{d}d)/\sqrt{2}$, and glueball. The dots represent the averaged values of each component, and the error bars reflect the uncertainties of $m^{\text{expt}}[f_0(600)]$ and $m^{\text{expt}}[f_0(1370)]$. The figures show that the components of $f_0(600)$, $f_0(980)$, and $f_0(1370)$ are not very sensitive to these experimental uncertainties, but some of the components of $f_0(1500)$ and $f_0(1710)$ (such as their glueball component) are significantly affected by such uncertainties.

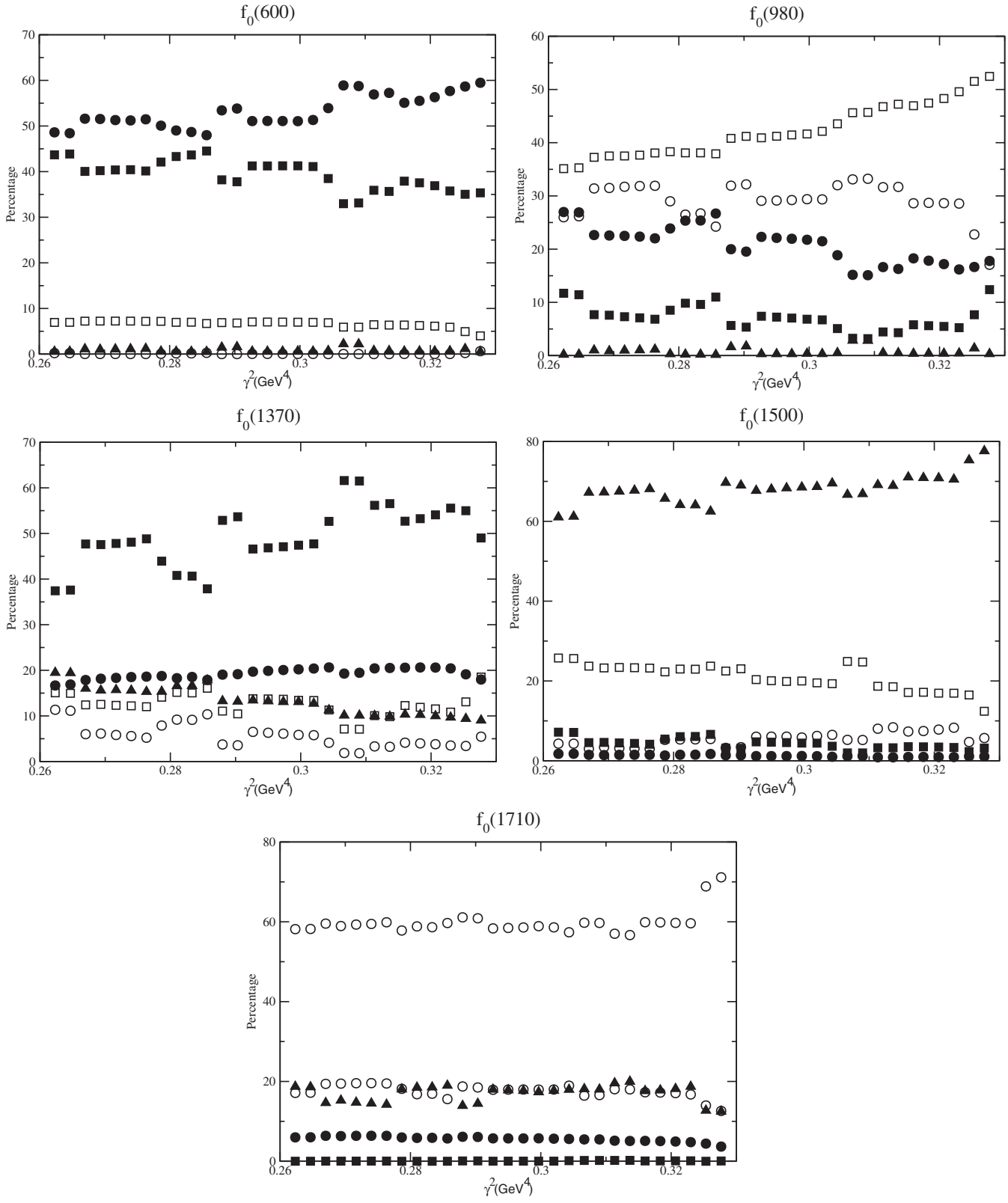

FIG. 9. Percentage of quark and glueball components of the scalar states vs γ^2: $\bar{u}\,\bar{d}\,ud$ (filled circles), $(\bar{s}\,\bar{d}\,ds + \bar{s}\,\bar{u}\,us)/\sqrt{2}$ (empty circles), $\bar{s}s$ (filled squares), $(\bar{u}u + \bar{d}d)/\sqrt{2}$ (empty squares), and glueball (filled triangles). The figures show that the components are not very sensitive to the mixing parameter γ.

$$m_G = \sqrt{2g} = 1.5 \rightarrow 1.7 \text{ GeV}. \quad (24)$$

At the local minima of Fig. 5, we compute the rotation matrix K^{-1} [defined in Eq. (13)] which maps the quark and glueball bases to the physical bases. The results show that K^{-1} is less sensitive to the masses of $f_0(600)$ and $f_0(1370)$. For each scalar state, the quark and glueball components versus $m^{\text{expt}}[f_0(600)]$ are given in Fig. 7, and the averaged components together with their variations are given in Fig. 8. Although the $m^{\text{expt}}[f_0(600)]$ is still over a wide range of 400 to 700 MeV, we see in Fig. 7 that some of the components of the physical state are qualitatively stable: The admixtures of $f_0(600)$, $f_0(980)$, and $f_0(1370)$, as well as some of the components of $f_0(1500)$ and $f_0(1710)$ are within a relatively small range of variation. We see that $f_0(600)$ has a dominant $\bar{u}\,\bar{d}\,ud$ component and some $\bar{s}s$ content, and it has almost the reverse structure of $f_0(1370)$; $f_0(980)$ is dominantly a two-quark nonstrange state $(\bar{u}u + \bar{d}d)$ with a significant strange four-quark content $(\bar{s}\,\bar{d}\,ds + \bar{s}\,\bar{u}\,us)$. Although sensitive to the masses of $f_0(600)$ and $f_0(1370)$, we see that $f_0(1500)$ contains a dominant glueball content with some strange four-quark and nonstrange two-quark admixtures; $f_0(1710)$ is a dominant strange four-quark state with a comparable glueball component.

IV. SUMMARY AND CONCLUSION

We studied the $I = 0$ scalar mesons below 2 GeV using a nonlinear chiral Lagrangian which is constrained by the mass and the decay properties of the $I = 1/2$ and $I = 1$ scalar meson below 2 GeV [$K_0^*(800)$, $K_0^*(1430)$, $a_0(980)$, and $a_0(1450)$]. This framework provides an efficient approach for predicting the quark and glueball content of the scalar mesons. The main obstacle for a complete prediction is the lack of an accurate experimental input for the masses of $f_0(600)$ and $f_0(1370)$. Nevertheless, we showed that several relatively robust conclusions can be made. We showed that $f_0(600)$, $f_0(980)$, and $f_0(1370)$ have a substantial admixture of two- and four-quark components with a negligible glueball component. The present model predicts that $f_0(600)$ is dominantly a nonstrange four-quark state; $f_0(980)$ has a dominant nonstrange two-quark component; and $f_0(1370)$ has a significant $\bar{s}s$ admixture. We also showed that this model predicts that $f_0(1500)$ and $f_0(1710)$ have considerable two- and four-quark admixtures, together with a dominant glueball component. The current large uncertainties on the masses of $f_0(600)$ and $f_0(1370)$ do not allow an exact determination of the glueball components of $f_0(1500)$ and $f_0(1710)$, but it is qualitatively clear that the glueball components of these two states are quite large. In addition, the present model predicts that the glueball mass is in the range 1.5–1.7 GeV [Eq. (24)].

The main theoretical improvement of the model involves the inclusion of higher order mixing terms among nonets N and N' and the scalar glueball:

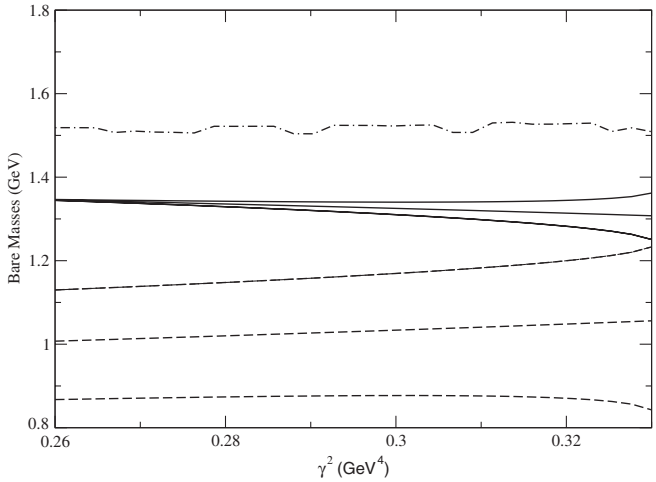

FIG. 10. Dependence of the bare masses on γ^2. The four-quark scalar nonet (dashed lines) lies below the quark-antiquark scalar nonet (solid lines) and a scalar glueball (dotted-dashed line).

$$\text{Tr}\,(\mathcal{M}NN') + \text{Tr}(\mathcal{M}N'N), \qquad \text{Tr}(\mathcal{M}N)\,\text{Tr}(N'),$$
$$\text{Tr}(\mathcal{M}N')\,\text{Tr}(N), \qquad G\,\text{Tr}(\mathcal{M}N), \qquad G\,\text{Tr}(\mathcal{M}N'). \quad (25)$$

However, these terms both mix the quarks and glueballs as well as break SU(3) symmetry, and therefore are of a more complex nature compared to the terms used in this investigation [Eqs. (6) and (9)]. Investigation of such higher order mixing terms will be left for future works. It is also important to note that the results presented here are not sensitive to the choice of γ which determines the mixing among the $I = 1/2$ and $I = 1$ mixings in Eq. (6). This is shown in Fig. 9 in which the components of all $I = 0$ states are plotted versus γ^2 and show that they are relatively stable. Also, in Fig. 10 the bare masses are plotted versus γ^2 in which we see that the expected ordering (i.e. the lowest-lying four-quark nonet N underlies a heavier two-quark nonet N' and a glueball), which is examined in Ref. [17] using the properties of the $I = 1/2$ and $I = 1$ scalar states, is not sensitive to the choice of mixing parameter γ, providing further support for the plausibility of the leading mixing terms considered in the present investigation.

ACKNOWLEDGMENTS

The author wishes to thank M. R. Ahmady, J. Schechter, and W. Thistleton for many helpful discussions. This work has been supported in part by a 2005–2006 Crouse Grant from the School of Arts and Sciences, SUNY Institute of Technology.

[1] S. Eidelman *et al.* (Particle Data Group), Phys. Lett. B **592**, 1 (2004).
[2] E. M. Aitala *et al.*, Phys. Rev. Lett. **89**, 121801 (2002).
[3] M. Ishida, Prog. Theor. Phys. Suppl. **149**, 190 (2003).
[4] C. Gobel, AIP Conf. Proc. **688**, 266 (2004).
[5] M. Ishida, AIP Conf. Proc. **688**, 18 (2004).
[6] M. Ablikim *et al.*, Phys. Lett. B **633**, 681 (2006).
[7] S. Kopp *et al.*, Phys. Rev. D **63**, 092001 (2001).
[8] S. Cherry and M. R. Pennington, Nucl. Phys. **A688**, 823 (2001).
[9] R. L. Jaffe, Phys. Rev. D **15**, 267 (1977).
[10] J. Weinstein and N. Isgur, Phys. Rev. D **41**, 2236 (1990).
[11] N. A. Törnqvist, Z. Phys. C **68**, 647 (1995); E. van Beveren *et al.*, Z. Phys. C **30**, 615 (1986).
[12] F. Sannino and J. Schechter, Phys. Rev. D **52**, 96 (1995); M. Harada, F. Sannino, and J. Schechter, Phys. Rev. D **54**, 1991 (1996); Phys. Rev. Lett. **78**, 1603 (1997).
[13] D. Black, A. H. Fariborz, F. Sannino, and J. Schechter, Phys. Rev. D **58**, 054012 (1998).
[14] D. Black, A. H. Fariborz, F. Sannino, and J. Schechter, Phys. Rev. D **59**, 074026 (1999).
[15] A. H. Fariborz and J. Schechter, Phys. Rev. D **60**, 034002 (1999).
[16] D. Black, A. H. Fariborz, and J. Schechter, Phys. Rev. D **61**, 074030 (2000).
[17] D. Black, A. H. Fariborz, and J. Schechter, Phys. Rev. D **61**, 074001 (2000).
[18] D. Black, A. H. Fariborz, S. Moussa, S. Nasri, and J. Schechter, Phys. Rev. D **64**, 014031 (2001).
[19] D. Black, M. Harada, and J. Shechter, Phys. Rev. Lett. **88**, 181603 (2002); Phys. Rev. D **73**, 054017 (2006).
[20] A. Abdel-Rahim, D. Black, A. H. Fariborz, S. Nasri, and J. Schechter, Phys. Rev. D **68**, 013008 (2003).
[21] A. Abdel-Rahim, D. Black, A. H. Fariborz, and J. Schechter, Phys. Rev. D **67**, 054001 (2003).
[22] A. H. Fariborz, Int. J. Mod. Phys. A **19**, 2095 (2004).
[23] A. H. Fariborz, Int. J. Mod. Phys. A **19**, 5417 (2004).
[24] A. H. Fariborz, R. Jora, and J. Schechter, Phys. Rev. D **72**, 034001 (2005).
[25] V. Elias, A. H. Fariborz, Fang Shi, and T. G. Steele, Nucl. Phys. **A633**, 279 (1998); Fang Shi, T. G. Steele, V. Elias, K. B. Sprague, Ying Xue, and A. H. Fariborz, Nucl. Phys. **A671**, 416 (2000).
[26] M. Boglione and M. R. Pennington, Phys. Rev. D **65**, 114010 (2002).
[27] T. Kunihiro, S. Muroya, A. Nakamura, C. Nonaka, M. Sekiguchi, and H. Wada, Phys. Rev. D **70**, 034504 (2004).
[28] T. Umekawa, K. Naito, M. Oka, and M. Takizawa, Phys. Rev. C **70**, 055205 (2004).
[29] L. Maiani, F. Piccinini, A. D. Polosa, and V. Riquer, Phys. Rev. Lett. **93**, 212002 (2004).
[30] T. Teshima, I. Kitamura, and N. Morisita, Nucl. Phys. **A759**, 131 (2005).
[31] H. Y. Cheng, C. K. Chua, and K. C. Yang, Phys. Rev. D **73**, 014017 (2006).
[32] Yu. Kalashnikova, A. Kudryavtsev, A. V. Nefediev, J. Haidenbauer, and C. Hanhart, Phys. Rev. C **73**, 045203 (2006).
[33] N. N. Achasov and A. V. Kiselev, Phys. Rev. D **73**, 054029 (2006).
[34] C. McNeile and C. Michael, Phys. Rev. D **74**, 014508 (2006).
[35] E. van Beveren, J. Costa, F. Kleefeld, and G. Rupp, Phys. Rev. D **74**, 037501 (2006).
[36] N. A. Törnqvist, hep-ph/0606041.
[37] P. Monkowski and W. Ochs, Eur. Phys. J. C **9**, 283 (1999).
[38] F. E. Close and A. Kirk, Phys. Lett. B **483**, 345 (2000).
[39] F. Close and N. Tornqvist, J. Phys. G **28**, R249 (2002).
[40] T. Teshima, I. Kitamura, and N. Morisita, J. Phys. G **28**, 1391 (2002).
[41] T. Teshima, I. Kitamura, and N. Morisita, J. Phys. G **30**, 663 (2004).
[42] M. Napsuciale and S. Rodriguez, Phys. Rev. D **70**, 094043 (2004).
[43] J. Vijande, A. Valcarce, F. Fernandez, and B. Silvestre-Brac, Phys. Rev. D **72**, 034025 (2005).
[44] S. Narison, Phys. Rev. D **73**, 114024 (2006).
[45] F. Giacosa, T. Gutsche, and A. Faessler, Phys. Rev. C **71**, 025202 (2005).
[46] T. V. Brito, F. S. Navarra, M. Nielsen, and M. E. Bracco, Phys. Lett. B **608**, 69 (2005).
[47] F. Giacosa, Th. Gutsche, V. E. Lyubovitskij, and A. Faessler, Phys. Lett. B **622**, 277 (2005).
[48] F. Giacosa, Phys. Rev. D **74**, 014028 (2006).
[49] L. Maiani, F. Piccinini, A. D. Polosa, and V. Riquer, hep-ph/0604018.
[50] The overall completion of the numerical analysis of this article required several months of computation time on a XEON dual-processor workstation.
[51] N. Ishii, H. Suganuma, and H. Matsufuru, Phys. Rev. D **66**, 014507 (2002); Xi-Yan Fang, Ping Hui, Qi-Zhou Chen, and D. Schutte, Phys. Rev. D **65**, 114505 (2002); C. J. Morningstar and M. Peardon, Phys. Rev. D **60**, 034509 (1999); J. Sexton, A. Vaccarino, and D. Weingarten, Phys. Rev. Lett. **75**, 4563 (1995); G. Bali *et al.*, Phys. Lett. B **309**, 378 (1993).